

Chapter 3

Design of Piezoelectric Actuators with Guaranteed Performances Using the Performances Inclusion Theorem

Micky Rakotondrabe and Sofiane Khadraoui

Abstract This chapter presents the design of piezoelectric actuators by using the performances inclusion theorem (PIT). The main objective is to seek for the dimensions of a cantilevered actuator such that its performances will lie within some specifications imposed *a priori*. For that, these specifications are transcribed into an interval transfer function, called interval reference model, while an interval model of the actuator is also provided. Then, from the PIT, a problem of finding the dimensions is yielded such that this latter model is enclosed in the reference model. The problem is seen as a set-inversion problem that can be solved with interval tools such as the SIVIA (Set Inversion Via Interval Analysis) algorithms. The designed piezoelectric actuator is afterwards fabricated and characterized. The experimental characterizations demonstrate the efficiency of the proposed technique.

3.1 Introduction

Piezoelectric materials are well recognized for the design and development of actuators in systems working at the micro/nanoscale, in particular for micro/nanopositioning systems. This recognition is due to their high bandwidth, high resolution and high density force. Furthermore, the fact that they can be used for sensing and actuation and the fact that their energy control is electrical make them more attractive than thermal or other active or smart materials.

M. Rakotondrabe (✉)

Automatic Control and Micro-Mechatronic Systems Department, AS2M,
FEMTO-ST Institute, 24 rue Alain Savary, Besançon 25000, France
e-mail: mrakoton@femto-st.fr

S. Khadraoui

Texas A&M University at Qatar, PO Box 23874, Education city, Doha, Qatar
e-mail: khadraoui.s@hotmail.fr

In micro/nanopositioning, there are several approaches to use piezoelectric materials: stepper piezoelectric actuators such as stick-slip or inch-worm motion principle [1–4], ultrasonic piezoelectric actuators [5–7], and flexible and continuously deformed piezoelectric cantilevers used in microgrippers or in microscopes [8–10]. In the fields of micromanipulation and microassembly, piezoelectric cantilever actuators with rectangular section are often used to develop microgrippers able to pick, transport, and place precisely small objects. These piezoelectric cantilevered structures offer an ease of control of the force or of the deflection (position of the object) which is essential when performing precise positioning and manipulation at the same time.

In general, the design of piezoelectric cantilevered actuators are done without explicit and *a priori* information on desired performances. Then, the designed actuators often offer any performances to which the applications should adapt instead of the converse, i.e. instead of designing actuators that would fit with the applications. Recently, an optimal design technique was proposed in [11] to design piezoelectric systems. Based on the gramian tools in control theory, the technique can provide optimal locations of cantilevered piezoelectric actuators and sensors. In this sense, the technique is useful when the system is based on several cantilevers such as treillis and then cannot be used for one cantilever-based system that are used in microgrippers. The aim of this chapter is to propose a novel technique to design piezoelectric cantilever-based actuators and systems. The main difference relative to the work in [11] is that we can design systems with single cantilevered actuators. Furthermore, in the proposed technique, we impose *a priori* some desired performances and specifications. For that, we propose to use interval tools, in particular we will use the performances inclusion theorem (PIT) developed in [12] which is effectively an efficient tool to also design actuators.

Interval tools [13, 14] are techniques that were efficiently used in different applications: control theory and control systems, robotics, signals and parameters estimation, etc. The main advantage of interval tools is the *guarantee* aspect that they can offer with the results, i.e. guaranteed solution or guaranteed nonsolution. In this chapter, we propose to benefit from such advantage to find guaranteed dimensions of piezoelectric actuators that would provide some specified performances. The chapter is organized as follows.

In Sect. 3.2, some preliminaries on intervals techniques are given. The PIT is particularly reminded. Section 3.3 is devoted to the modeling of piezoelectric cantilevered actuators. Models of multilayered actuators are treated in both static and dynamics. In Sect. 3.4, the novel technique to design piezoelectric actuators is proposed. We particularly focus on the design of unimorph cantilevered actuators. Finally, fabrication and experimental tests on the fabricated actuators are carried out which demonstrate the efficiency of the proposed approach.

3.2 Preliminaries on Intervals

3.2.1 Definitions

We remind here some basics on intervals that will be used in the rest of the chapter. The readers who are interested to see more in details the techniques of intervals are suggested to read the references [13, 14].

A real interval $[x]$ is a closed interval such that:

$$[x] = [x^-, x^+] \quad (3.1)$$

where x^- and x^+ are called lower bound and upper bound, respectively. We have: $x^- \leq x^+$. Having $x^- = x^+$ means that the interval $[x]$ is degenerate. By convention, a degenerate interval $[a] = [a, a]$ is identified by the real number a . The designation *point number* is similar to the designation *degenerate interval number*. While the set of real point numbers is \mathbb{R} , the set of real intervals (or real interval numbers) is \mathbb{IR} .

Instead of using the notation in (3.1), one can also identify a real interval number by its midpoint $\text{mid}([x])$ and its radius $\text{rad}([x])$ such that:

$$\begin{cases} \text{mid}([x]) = \frac{(x^+ + x^-)}{2} \\ \text{rad}([x]) = \frac{(x^+ - x^-)}{2} = \frac{w([x])}{2} \end{cases} \quad (3.2)$$

where $w([x])$ is the width of the interval.

3.2.2 Operations on Intervals

In the arithmetics of intervals, the basic operations are extended to interval numbers. Consider two intervals $[x] = [x^-, x^+]$ and $[y] = [y^-, y^+]$. So we have:

$$[x] + [y] = [x^- + y^-, x^+ + y^+] \quad (3.3)$$

and

$$[x] - [y] = [x^- - y^+, x^+ - y^-] \quad (3.4)$$

Consequently, we have: $[x] - [x] \neq 0$, except for $x^- = x^+$.

The multiplication and division are defined as follows:

$$[x] \cdot [y] = [\min(x^-y^-, x^-y^+, x^+y^-, x^+y^+), \max(x^-y^-, x^-y^+, x^+y^-, x^+y^+)] \quad (3.5)$$

and

$$[x] / [y] = [x] \cdot [1/y^+, 1/y^-], 0 \notin [y] \quad (3.6)$$

We say that an interval $[x]$ is included in an interval $[y]$, i.e. $[x] \subset [y]$, if and if only $[x] \cap [y] = [x]$. We have $[x] > [y]$ if $x^- > y^+$. The real interval $[x]$ is said to be positive if $x^- > 0$. The distributive law does not hold in general for interval. However, the following relation, called subdistributivity, holds: $[x]([y] + [z]) \subseteq [x][y] + [x][z]$. In addition, if $[x] + [y] = [x] + [z]$, the cancellation law for addition holds, and $[y] = [z]$. The same property holds for multiplication: if $[x][y] = [x][z]$ and $0 \notin [x]$, thus $[y] = [z]$.

If f is a function $f : \mathbb{R} \rightarrow \mathbb{R}$, then its interval counterpart $[f]$ satisfies:

$$[f]([x]) = [\{f(x) : x \in [x]\}] \quad (3.7)$$

The interval function $[f]$ is called inclusion function because $f([x]) \subseteq [f]([x])$, for all $[x] \in \mathbb{IR}$. An inclusion function $[f]$ is thin if for any degenerate interval $[x] = x$, $[f](x) = f(x)$. It is minimal if for any $[x]$, $[f]([x])$ is the smallest interval that contains $f([x])$. The minimal inclusion function for f is unique and is denoted by $[f]^*([x])$.

An easy way to compute an inclusion function for f is to replace each variable x in the expression of f by $[x]$ and all operations on points by their interval counterpart. Thus, one obtains the natural inclusion function.

3.2.3 Interval Systems

An interval system is a transfer function representation, a state space representation or a differential representation where the parameters are intervals. For an interval transfer function, which is the interest of this chapter, the representation is as follows:

$$[G](s) = \frac{[b_m]s^m + \dots + [b_1]s^1 + [b_0]}{[a_n]s^n + \dots + [a_1]s^1 + [a_0]} = \frac{\sum_{l=0}^m [b_l]s^l}{\sum_{k=0}^n [a_k]s^k} \quad (3.8)$$

where s is the Laplace variable and where $m \leq n$, n being the order of the interval system $[G](s)$. The parameters $[a_k]$ and $[b_l]$ are considered to be constant real intervals in order to assume linear time invariant (LTI) systems. The notation $[G](s)$ shall be used if the intervals $[a_k]$ and $[b_l]$ are known. Instead, the notation $[G]([a_k], [b_l], s)$ is used when they are unknown and to be sought for.

The notion of inclusion of systems should also be defined. Consider two interval systems having the same polynomials degrees m and n , i.e. having the same structure:

$$[G_1](s) = \frac{\sum_{l=0}^m [b_{1l}]s^l}{\sum_{k=0}^n [a_{1k}]s^k}, \quad [G_2](s) = \frac{\sum_{l=0}^m [b_{2l}]s^l}{\sum_{k=0}^n [a_{2k}]s^k} \quad (3.9)$$

$[G_1](s) \subseteq [G_2](s)$ is equivalent to saying that for any $s \in [0, \infty)$, we have $[G_1] \subseteq [G_2]$.

Lemma 2.1. *If $[b_{1l}] \subseteq [b_{2l}]$ and $[a_{1k}] \subseteq [a_{2k}]$, $\forall k, l$, then $[G_1](s) \subseteq [G_2](s)$.*

Proof. See [12].

3.2.4 The Performances Inclusion Theorem [12]

Consider two interval systems having the same polynomial degrees m and n :

$$[G_1](s) = \frac{\sum_{l=0}^m [b_{1l}] \cdot s^l}{\sum_{k=0}^n [a_{1k}] \cdot s^k}, \quad [G_2](s) = \frac{\sum_{l=0}^m [b_{2l}] \cdot s^l}{\sum_{k=0}^n [a_{2k}] \cdot s^k} \quad (3.10)$$

The PIT which will be used to further design actuators is composed of two results.

Theorem 2.1. *The performances inclusion in the frequency domain:*

$$\begin{aligned} \text{if } & \begin{cases} [a_{1k}] \subseteq [a_{2k}], \forall k = 1, \dots, n \\ \text{and} \\ [b_{1l}] \subseteq [b_{2l}], \forall l = 1, \dots, m \end{cases} \\ \Rightarrow & \begin{cases} [\rho]([G_1](j\omega)) \subseteq \rho([G_2](j\omega)) \\ \text{and} \\ [\varphi]([G_1](j\omega)) \subseteq \varphi([G_2](j\omega)) \end{cases} \end{aligned}$$

Theorem 2.2. *The performances inclusion in the time domain:*

$$\begin{aligned} \text{if } & \begin{cases} [a_{1k}] \subseteq [a_{2k}], \forall k = 1, \dots, n \\ \text{and} \\ [b_{1l}] \subseteq [b_{2l}], \forall l = 1, \dots, m \end{cases} \\ \Rightarrow & [g_1](t) \subseteq [g_2](t) \end{aligned}$$

where:

- $[\rho]([G_i](j\omega))$ is the modulus of the system $[G_i]$.
- $[\varphi]([G_i](j\omega))$ is the argument.
- $[g_i](t)$ is the impulse response.

Proof. See [12].

3.3 Piezoelectric Cantilevered Actuators and Their Modeling

3.3.1 Presentation of a Piezoelectric Cantilevered Actuator

A piezoelectric cantilevered actuator, alternately called piezocantilever, is a cantilever having one or several layers, where at least one layer is piezoelectric material. We are interested here by a cantilever with rectangular section. When the cantilever has many layers, it is called multilayered piezoelectric actuator. Often, if there are p piezoelectric layers in a multilayered cantilever, we also call the actuator a p -morph actuator [15]. In the actuator, the non-piezoelectric layers are called passive layers. They can be silicone, nickel, copper, chrome, polymer materials, etc. The objective with the actuator is that, when a voltage is applied to the piezoelectric layers, the whole cantilever bends. Figure 3.1a presents a multilayered piezoelectric actuator with n layers. In Fig. 3.1b, a bilayer unimorph piezoelectric actuator is presented. The application of a voltage U to the piezoelectric layer makes it contract/expand resulting a global deflection of the cantilever. In Fig. 3.1c, a bilayer bimorph actuator is depicted. The application of the voltage U , yielding an electrical field parallel and anti-parallel to the internal polarization P_{0i} of the two layers yields a contraction and a compression of them. This antagonist longitudinal deformation yields a bending of the cantilever.

An unimorph actuator is more simple to develop and to use, in particular in terms of electrical connection. A bimorph actuator (and a multimorph actuator) is more complex to settle. However, relative to an unimorph actuator, it offers higher deformation and bending with the same applied voltage.

3.3.2 Static Model

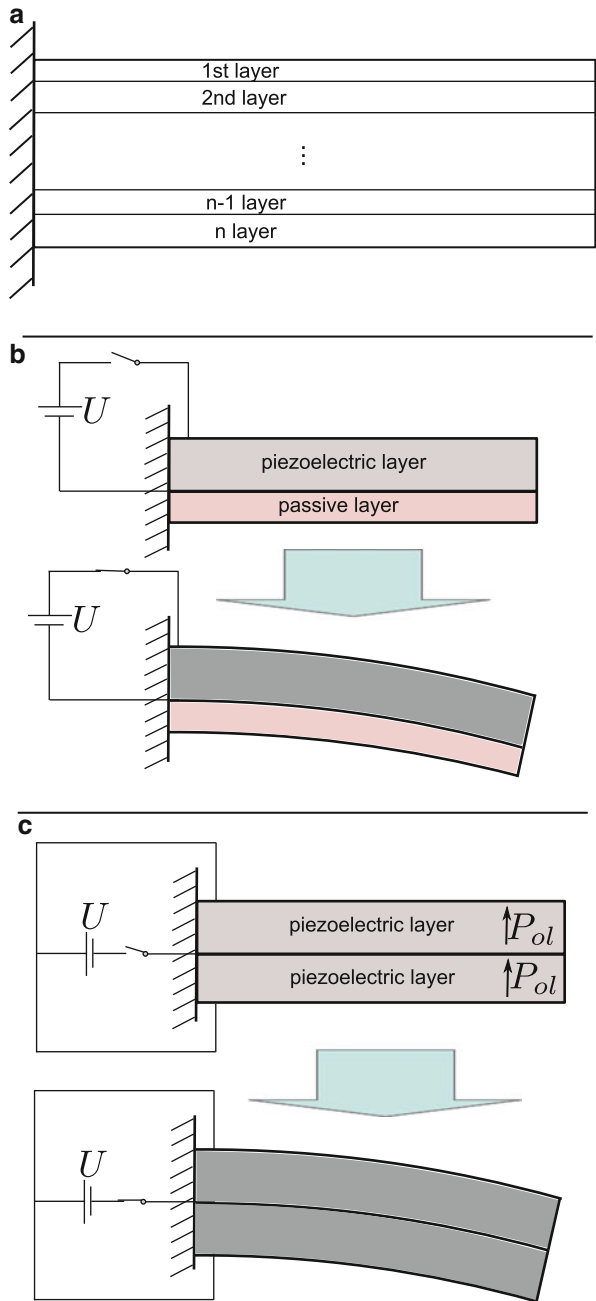
First, the static model of a multilayered piezoelectric cantilever is given. We are particularly interested in the resulting deflection of the actuator when a voltage is applied. Consider the n -layered actuator pictured in Fig. 3.2a where:

- h_i , with $i \in \{1, 2, \dots, n\}$, is the i th layer.
- \bar{y} is the distance between the neutral fiber and the bottom surface of the cantilever.

Each layer of the cantilever is exclusively a piezoelectric material or a passive material. The only rule is that at least one layer among the i -layers is piezoelectric. The application of a voltage U to the piezoelectric layers yields a bending of the whole cantilever as depicted in Fig. 3.2b. The bending $y(x)$ at distance x from the clamp can be written as follows [16]:

$$y(x) = \frac{m_{\text{piezo}} x^2}{2C} U \quad (3.11)$$

Fig. 3.1 (a): a multilayered piezoelectric cantilever.
 (b): a (bilayer) unimorph piezoelectric cantilever.
 (c): a (bilayer) bimorph piezoelectric cantilever



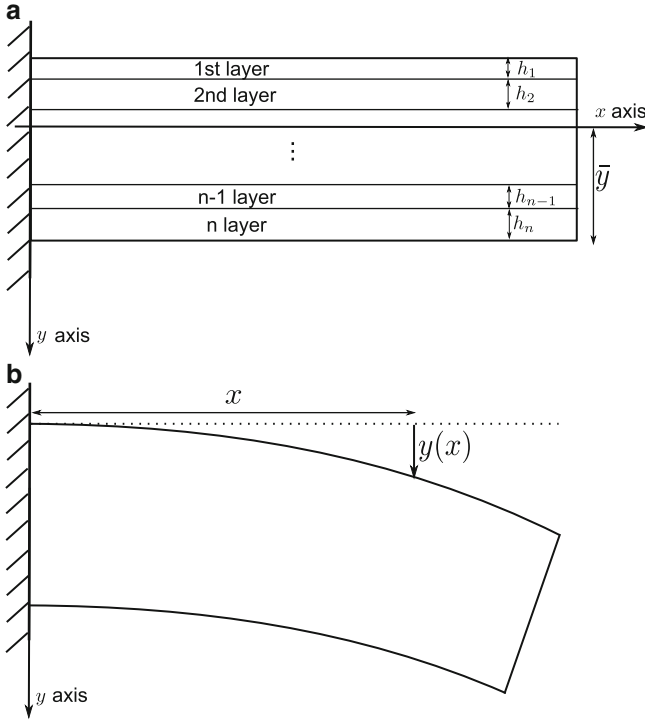


Fig. 3.2 (a): a multilayered piezoelectric cantilever. (b): bending of a multilayered piezoelectric cantilever

with

$$\begin{cases} m_{\text{piezo}} = \frac{1}{2} \sum_{i=1}^n \frac{w_i d_{31,i}}{s_{11,i} h_i} \left[2\bar{y} h_i - 2h_i \sum_{j=1}^i h_j + h_i^2 \right] \\ C = \frac{1}{3} \sum_{i=1}^n \frac{w_i}{s_{11,i}} \left[3h_i \left(\bar{y} - \sum_{j=1}^i h_j \right) \left(\bar{y} - \sum_{j=1}^{i-1} h_j \right) + h_i^2 \right] \end{cases} \quad (3.12)$$

where

- w_i is the width of the i th layer. In the sequel, it is assumed that $w_i = w$, $\forall i \in \{1, 2, \dots, n\}$.
- $d_{31,i}$ is the transversal piezoelectric coefficient of the i th layer. If the layer is non-piezoelectric material, i.e. passive material, we have $d_{31,i} = 0$.
- $s_{11,i}$ is the elastic coefficient.

At the tip of the cantilever, this bending is

$$y(x=L) = y = \frac{m_{\text{piezo}} L^2}{2C} U \quad (3.13)$$

where L is the length of the cantilever.

Table 3.1 Numerical value of $k_m L$

m	1	2	3	4	5	...
$k_m L$	1.8751	4.6941	7.8548	10.9955	14.137	...

3.3.3 Dynamic Model

The previous model is static and relates the steady-state deflection $y(x)$ of the cantilever when a voltage U is applied. For performances and control point of view, a static model is insufficient, and it is important to also have an idea of the dynamics of the actuator. An essential parameter that can describe the dynamics of a system is the resonant frequency if the system is oscillating, which is the case for cantilevered actuators in general. A high resonant frequency indicates that it has a large bandwidth. For a multimorph piezoelectric cantilevered actuator, the m th resonant frequency $f_m [Hz]$ is defined as follows [16]:

$$f_m = \frac{(k_m L)^2}{2\pi L^2} \sqrt{\frac{C}{\mu}} \quad (3.14)$$

where C is defined by (3.12) and k_m is called wave number and can be calculated from the Table 3.1. The coefficient μ is given by:

$$\mu = \frac{M}{L} = \sum_{i=1}^n \rho_i h_i w_i \quad (3.15)$$

such that M is the mass of the cantilever, L being its length, and ρ_i is the density of the i th layer.

It is noticed, however, that there is no analytical solution to determine the damping ratio associated with each mode. In general, this is provided experimentally.

3.3.4 Equivalent Parametric Model

In order to design a piezoelectric actuator that will satisfy some specified performances, we will use the previous static model augmented with the resonant frequency information. The previous model is general: it provides the deflection at any point x along the cantilever and all resonant frequencies (until to the m th mode) are given. In our applications, we are interested in the deflection at the tip, i.e. for $x = L$, which is the most useful. Indeed, the manipulation of objects is often performed with the extremity of the cantilever. In addition, the first resonant frequency $m = 1$ is sufficient. We therefore provide a model limited to the first mode and where the range of deflection is calculated at the tip of the cantilevered actuator. Such a model is a second order model that is expressed by the following transfer function:

$$G(s) = \frac{Y(s)}{U(s)} = \frac{K}{\frac{1}{(w_n)^2}s^2 + \frac{2\xi}{w_n}s + 1} \quad (3.16)$$

where:

- s is the Laplace variable.
- $G(s)$ is the name of the model.
- $Y(s)$ and $U(s)$ are the Laplace transforms of $y(t)$ and $U(t)$, respectively.
- K is the statical gain.
- $w_n[\frac{\text{rad}}{s}]$ is the natural frequency.
- ξ is the damping ratio.

The statical gain K is derived from (3.13):

$$K = \frac{Y(s \rightarrow 0)}{U(s \rightarrow 0)} = \frac{y(t \rightarrow \infty)}{U(t \rightarrow \infty)} = \frac{m_{\text{piezo}}L^2}{2C} \quad (3.17)$$

The natural frequency is dependent on the damping ratio ξ and on the first resonant frequency $[\frac{\text{rad}}{s}]$ as described as follows:

$$w_n = \frac{w_r}{\sqrt{1 - 2\xi^2}} \quad (3.18)$$

with $w_r[\frac{\text{rad}}{s}] = 2\pi f_1$ and such that f_1 is calculated from (3.14) by letting $m = 1$. We have:

$$f_1 = \frac{(1.8751)^2}{2\pi L^2} \sqrt{\frac{C}{\mu}} \quad (3.19)$$

Remind that the damping ratio ξ is not defined analytically. Hence, we cannot use this as (extra-)parameter for the design.

In the sequel, we are interested in designing unimorph piezocantilever, i.e. a cantilever made up of two layers: one piezoelectric layer and one passive layer. Hence, the coefficients C and m_{piezo} we have in (3.17) and (3.19) are calculated by setting $n = 2$ in (3.12) and by using the coefficients of the materials used. We have:

$$\begin{cases} m_{\text{piezo}} = \frac{-wd_{31}h_{mp}(h_p+h_{mp})}{2(s_{11}^{mp}h_p+s_{11}^p h_{mp})} \\ C = \frac{w[(s_{11}^p)^2 h_{mp}^4 + s_{11}^{mp} s_{11}^p (4h_p h_{mp}^3 + 6h_p^2 h_{mp}^2 + 4h_{mp} h_p^3) + (s_{11}^{mp})^2 + h_p^4]}{12s_{11}^{mp} s_{11}^p (s_{11}^{mp} h_p + s_{11}^p h_{mp})} \end{cases} \quad (3.20)$$

where:

- d_{31} is the transversal piezoelectric coefficient, h_p is the thickness, and s_{11}^p is the elastic coefficient of the piezoelectric layer.
- h_{mp} is the thickness and s_{11}^{mp} is the elastic coefficient of the passive material.

3.4 Design of a Unimorph Piezoelectric Actuator by Using the PIT

This section presents a methodology for designing piezoelectric cantilevered actuators by combining the analytical modeling presented in the previous section and interval techniques. We are particularly interested in the design of unimorph piezoelectric actuators. This choice is motivated by the ease of their fabrication and of electrical connection with respect to that of the bimorph and multimorph piezocantilevers. The design problem is formulated as a set inversion problem which is then solved using interval techniques. The proposed design technique is novel and very interesting in the sense that the design yields guaranteed performances, if solution exists.

3.4.1 Specifications

We aim to design unimorph piezocantilevers for which some desired performance specifications given either in the time domain or in the frequency domain should be met. These specifications can be transcribed into a model, called reference model, i.e. is a transfer function or a state-space representation. Considering bounded performance measures, the model parameters are also bounded. Taking therefore a reference model with the same structure than the system model in (3.16) (second order model), we consider the following reference (or desired) model where the parameters are intervals:

$$[G_d](s, [p]) = \frac{[a_0]}{[a_2]s^2 + [a_1]s + 1} \quad (3.21)$$

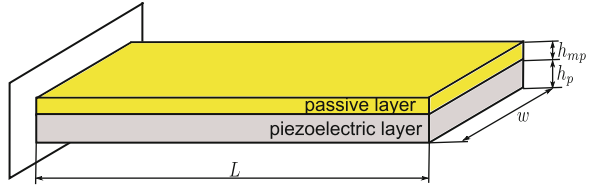
such that $[p] = ([a_0], [a_1], [a_2])^T$ is a vector of interval parameters that can be derived from the specified performances. The unit step response of (3.21) defines upper and lower envelopes of the desired step response. Also, the interval magnitude and phase of (3.21) over a sufficient set of frequencies defines upper and lower bounds of the desired frequency response [12].

3.4.2 Problem Formulation

Reconsider a unimorph piezocantilever having a length L , width w , and thicknesses h_p and h_{mp} for its piezoelectric and passive layers, respectively, as reminded in Fig. 3.3.

As shown in previous section, the static and dynamic models of the unimorph piezocantilever depend on the geometrical sizes and the physical properties of

Fig. 3.3 Unimorph piezocantilever



the materials that compose it. The model that relates this fact is given by (3.16). If we admit that, for given piezoelectric and passive materials, there is a set of dimensions (i.e., of the length, of the thicknesses, and of the width) that would provide performances which lie within the specified performances transcribed by (3.21), these geometrical sizes can also be described by intervals. These interval geometrical parameters yield therefore interval model parameters and the initial model in (3.16) becomes an interval model as follows:

$$[G](s, [q]) = \frac{[K]}{\frac{1}{[w_n]^2} s^2 + \frac{2[\xi]}{[w_n]} s + 1} \quad (3.22)$$

where $[q] = ([K], [w_n], [\xi])^T$ is a vector containing the interval static gain $[K]$, the interval natural frequency $[w_n]$ and the interval damping ratio $[\xi]$. $[K]$ and $[w_n]$ can be easily derived using the geometrical sizes and physical properties of the unimorph piezoelectric actuator as presented in Sect. 3.3.

According to (3.17) and (3.19), the resonant frequency of a unimorph piezocantilever is conversely proportional to the square of its length whereas the deflection is directly proportional to the square of its length. Therefore, decreasing the length results in increasing the resonant frequency and therefore enlarging the bandwidth. However, the static gain will be reduced and the range of deflection will be limited. This decrease in the range can be compensated by some setting on the thicknesses of the piezoelectric and passive layers, while holding a large bandwidth. For that, our endeavor consists in finding the best geometrical sizes of the unimorph piezocantilever such that its performance still satisfies the specified performances that are described by the interval reference model (3.21). Such a problem can be formulated as follows: for a pre-selected value of the damping ratio $[\xi] = \xi$, find suitable values of geometrical sizes with which the unimorph piezocantilever model is included in the interval reference model as follows:

$$[G](s, [q]) \subseteq [G_d](s, [p]) \quad (3.23)$$

The statement in (3.23) is from the PIT presented in Theorems 2.1 and 2.2. This statement tells us to find a set of geometrical sizes of unimorph cantilevers such that the performances of the corresponding model, denoted $[G]$, are enclosed in that of the reference model $[G_d]$.

In general, the applications (micromanipulation, microassembly, etc.) require that the width $[w]$ is imposed. Indeed, the maximal sizes of the manipulable objects with the actuator depend on this width. Therefore, in the sequel we fix $[w] = w$. Then, the remaining parameters to be sought for are the length $[L]$ and the thicknesses $[h_p]$ and $[h_{mp}]$. Let $[\theta] = ([L], [h_p], [h_{mp}])^T$ be an interval vector containing these design parameters. Now, our design problem consists in finding the possible values for the parameter $[\theta]$ for which the inclusion (3.23) is satisfied. To check the fulfillment of the inclusion $[G](s, [q]) \subseteq [G_d](s, [p])$ one can perform parameter by parameter inclusion as given in Lemma 2.1. Let Θ be the set corresponding to admissible values of the parameter $[\theta]$ for which (3.23) holds. Thus, the design problem to be addressed can be viewed as finding the set Θ so that:

$$\Theta := \left\{ \theta \in \mathcal{D} \left| \begin{array}{l} [K]([\theta]) \subseteq [a_0] \\ \frac{1}{([w_n]([\theta]))^2} \subseteq [a_2] \\ \frac{2\xi}{[w_n]([\theta])} \subseteq [a_1] \end{array} \right. \right\} \quad (3.24)$$

where \mathcal{D} is the definition domain of $[\theta]$. The problem (3.24) is known as a set-inversion problem and a possible way to solve a set-inversion problem is the SIVIA algorithm. In the next subsection, we introduce this algorithm to solve our design problem.

3.4.3 Solution Computation via the SIVIA Algorithm

The SIVIA algorithm [14, 17] is an interval technique that can be used to solve a set-inversion problem such as that of problem (3.24). The set inversion operation consists in computing the reciprocal image of a compact set called subpaving. The set-inversion algorithm SIVIA allows to solve the design problem given in (3.24) and provides an approximation with subpavings of the set solution Θ . This approximation is realized with an inner and outer subpavings, respectively, $\underline{\Theta}$ and $\overline{\Theta}$, such that $\underline{\Theta} \subseteq \Theta \subseteq \overline{\Theta}$. The subpaving Θ corresponds to geometrical sizes of the unimorph piezocantilever for which the problem (3.24) holds. If $\Theta = \emptyset$, then it is guaranteed that no solution exists for the design problem (3.24).

We provide in Table 3.2 the recursive SIVIA algorithm that allows to solve the design problem (3.24) with guaranteed solution. SIVIA algorithm requires a search box $[\theta_0]$ (possibly very large), also called initial box within which $\overline{\Theta}$ is guaranteed to belong. The inner and outer subpavings ($\underline{\Theta}$ and $\overline{\Theta}$) are initially empty. ε represents the wanted accuracy of computation.

Quite often we are interested to compute an inner approximation $\underline{\Theta}$ for which we are sure that $\underline{\Theta}$ is included in the set solution Θ , i.e., $\underline{\Theta} \subseteq \Theta$, but when no inner approximation exists i.e., $\underline{\Theta} = \emptyset$, it is possible to choose parameters inside the outer subpaving, i.e., choose $\theta \in \overline{\Theta}$.

Table 3.2 SIVIA algorithm for solving a set-inversion problem [14, 17]

Step	SIVIA(in: $[K], [w_n], [a_0], [a_1], [a_2], [\theta], \varepsilon$; inout: $\underline{\Theta}, \overline{\Theta}$)
1	if $\left(\frac{[K](\{\theta\})}{1} \right) \cap \left(\frac{[a_0]}{[a_2]} \right) = \emptyset$ return;
2	if $\left\{ \begin{array}{l} \frac{[K](\{\theta\}) \subseteq [a_0]}{1} \\ \wedge \\ \frac{2\xi}{[w_n](\{\theta\})} \subseteq [a_1] \end{array} \right\}$ then $\underline{\Theta} := \underline{\Theta} \cup \{\theta\}$ and $\overline{\Theta} := \overline{\Theta} \cup \{\theta\}$ return;
4	if $width([\theta]) < \varepsilon$ then $\{\overline{\Theta} := \overline{\Theta} \cup \{\theta\}\}$ return;
5	bisect $[\theta]$ into $L([\theta])$ and $R([\theta])$;
6	SIVIA($[K], [w_n], [a_0], [a_1], [a_2], L([\theta]), \varepsilon; \underline{\Theta}, \overline{\Theta}$); SIVIA($[K], [w_n], [a_0], [a_1], [a_2], R([\theta]), \varepsilon; \underline{\Theta}, \overline{\Theta}$).

Remark 1. The number of unknown parameters in (3.24) is 3 and the number of inclusions is also 3. The set solution Θ can be obtained by intersecting the set solution of each inclusion in (3.24), i.e.:

$$\Theta = \bigcap_{i=1}^3 (set_sol)_i$$

such as: $(set_sol)_i$ is the set solution of the i th inclusion.

Remark 2. If the set-inversion problem is not feasible, i.e. $\Theta = \emptyset$, the initial box of parameters must be changed and/or the desired performance specifications (interval reference model) must be relaxed.

3.4.4 Experimental Validation

This part is devoted to a numerical application and an experimental validation of the proposed design technique presented previously.

3.4.4.1 Materials

The layers of the unimorph to be designed are based on materials commercially available: a PZT-PIC151 (lead zirconate titanate) piezoelectric material from *Physike Instrumente* (PI) company for the piezoelectric layer and Nickel material

Table 3.3 Physical characteristics of PZT-PIC151 and of Nickel materials

Materials	Compliance s_{11}	Piezoelectric constant d_{31}	Density ρ
PZT	$15 \times 10^{-12} \text{ m}^2/\text{N}$	$-210 \times 10^{-12} \text{ m/V}$	$7,800 \text{ kg/m}^3$
Nickel	$5 \times 10^{-12} \text{ m}^2/\text{N}$	0	$8,900 \text{ kg/m}^3$

from *Goodfellow* company for the passive layer. The thermal glue “EPO-TEK H22” from *PI* is used to glue the piezoelectric and passive layers (PZT-Nickel). Table 3.3 summarizes some useful physical properties of the PZT-PIC151 and Nickel materials. These numerical values will be used during the design process of the unimorph piezocantilever.

3.4.4.2 Interval Reference Model

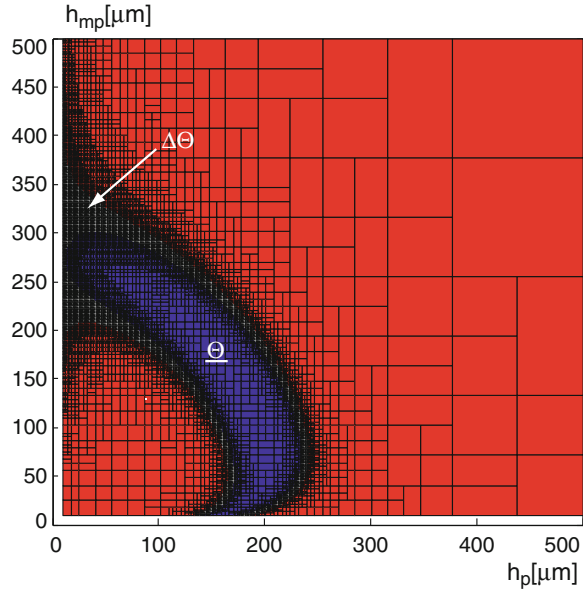
The reference model (3.21) is a transcription of some specifications. These specifications can be given in the time domain such as the settling time and the maximal overshoot, or in the frequency domain such as the resonant frequency. The relations that link these performances measures in the time domain or in the frequency domain with the coefficients $[a_0]$, $[a_1]$, and $[a_2]$ of a second order model will not be presented here. We directly give the following numerical values instead which, from our experience, corresponds to the performances required in our applications:

$$[G_d](s) = \frac{[0.5, 1]}{[0.156, 2.5] \times 10^{-7}s^2 + [0.25, 1] \times 10^{-5}s + 1} \quad (3.25)$$

3.4.4.3 Unimorph Sizes Computation

Our objective is now to design a unimorph piezocantilever having some performances that are enclosed in the performances of the interval reference model (3.25), i.e. finding the actuator’s sizes such that the model $[G]$ in (3.22) is enclosed in the reference model (3.25). The problem will be treated with a pre-fixed value of the damping ratio $[\xi] = \xi = 0.01$. In addition, in order to reduce the number of the design parameters, we set the unimorph piezocantilever length to $L = 16 \text{ mm}$ and its width to $w = 2 \text{ mm}$. At the end, our design problem boils down to find thicknesses $[h_p]$ and $[h_{mp}]$ of the piezoelectric and of the passive layers, respectively, so that inclusions (3.24) are satisfied. Using the numerical values defined so far and applying the SIVIA algorithm presented in Table 3.2 with an initial box $[h_p]_0 \times [h_{mp}]_0 = [10, 500] \times [10, 500]$ and an accuracy $\varepsilon = 1 \mu\text{m}$, we obtain the subpaving shown in Fig. 3.4. In this figure, the area denoted \mathcal{Q} corresponds to the guaranteed solution (inner subpaving), i.e. the set $[h_p] \times [h_{mp}]$ that satisfies the

Fig. 3.4 Set solution $\underline{\Theta}$ corresponding to the parameters h_p and h_{mp}



inclusion $[G](s) \subseteq [G_d](s)$. Any choice of the parameters $[h_p]$ and $[h_{mp}]$ within the subpaving $\underline{\Theta}$ ensures the inclusions problem given in (3.24). The area $\Delta\Theta$ contains the boxes for which no decision on the test of inclusion in (3.24) can be taken. Notice that:

$$\overline{\Theta} = \underline{\Theta} \cup \Delta\Theta$$

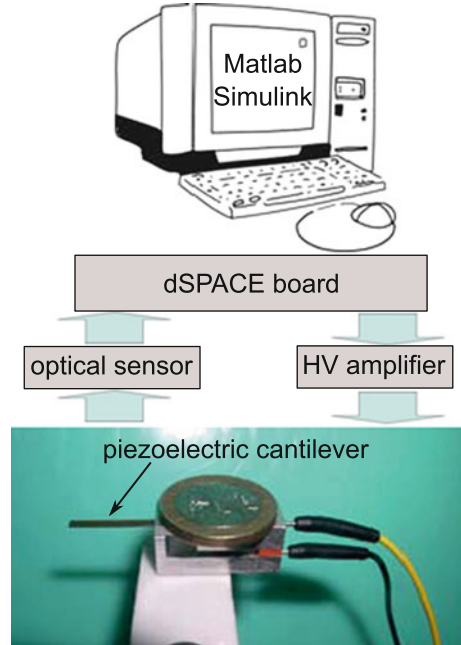
$\Delta\Theta$ can be minimized by increasing the computation accuracy. The remaining external boxes correspond to the parameters $[h_p]$ and $[h_{mp}]$ for which the inclusions (3.24) do not hold.

3.4.4.4 Fabrication of the Unimorph Piezocantilever and Experimental Verifications

In order to develop and fabricate some prototypes of unimorph piezocantilevers, we choose the following geometrical sizes:

$$\begin{cases} L = 16 \text{ mm} \\ h_p = 200 \mu\text{m} \\ h_{mp} = 100 \mu\text{m} \\ w = 2 \text{ mm} \end{cases} \quad (3.26)$$

Fig. 3.5 Prototype of a unimorph piezoelectric actuator and experimental setup

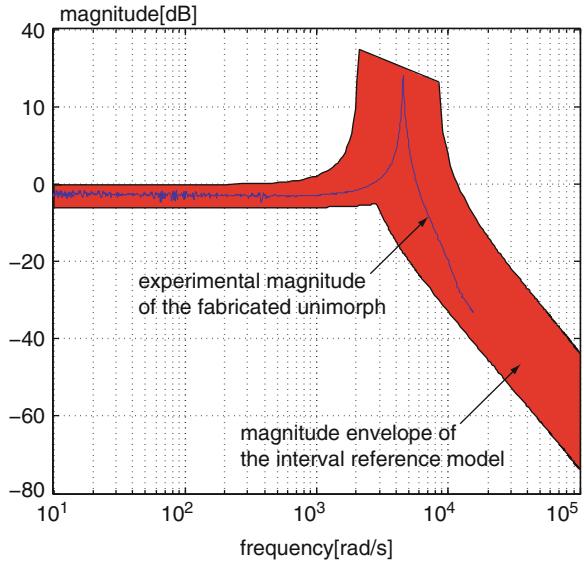


where h_p and h_{mp} have been chosen arbitrarily from the solution region Θ . Figure 3.5 presents a photography of the fabricated unimorph piezocantilever and the experimental setup. The whole experimental setup is composed of:

- The fabricated unimorph piezocantilever.
- An optical sensor (from *Keyence* company) with a resolution of 10 nm and used to measure the deflection of the piezocantilever.
- A high-voltage (HV) amplifier.
- A dSPACE acquisition board and a computer to generate the input voltage and to acquire the measurements. The sampling time of the whole acquisition system is set to 0.2 ms. The Matlab-Simulink software is used to manage the input and output signals.

In this application, the experimental verifications are done in the frequency domain. More precisely, we plot in the same graph the experimental frequency response of the designed piezocantilever and the frequency response of the reference model $[G_d]$. If the magnitude of the experimental response is enclosed in that of $[G_d]$, our objective is reached. For the experiment, we apply a sine input voltage with an amplitude of $U = 20\text{V}$ and a frequency ranging between 1 Hz ($6.28[\frac{\text{rad}}{\text{s}}]$) and more than 1,500 Hz ($9,500[\frac{\text{rad}}{\text{s}}]$) to the designed piezocantilever. The resulting experimental magnitude is shown in Fig. 3.6. In the same figure, the envelope magnitude that corresponds to the magnitude of the interval reference model is also plotted. According to Fig. 3.6, the experimental magnitude obtained with the

Fig. 3.6 Experimental magnitude of the unimorph and the desired magnitude



fabricated piezoelectric unimorph is enclosed in the desired magnitude of the interval reference model. Consequently, the method used to design a piezoelectric actuator by using the PIT efficiently provided the expected results and confirmed the theoretical results. Indeed, the performances obtained with the designed actuator lie within the performances imposed *a priori* as specifications.

3.5 Conclusion

In this chapter, the design of piezoelectric actuators based on the performance inclusion theorem has been presented. It has been shown that static and dynamic models of these piezoelectric actuators strongly depend on their geometrical sizes and physical properties. Then, our challenge was to design a (unimorph) piezoelectric actuator that would satisfy some imposed performances. Based on the inclusion performances theorem, the design problem has been formulated as a set-inversion problem. This later has been solved using interval techniques to find the geometrical sizes of the piezoelectric actuator. The main advantage of the proposed approach is that guaranteed solution or non-solution of the design problem can be obtained. The designed actuator was afterwards fabricated and characterized. The experimental results on the fabricated actuator validated the proposed method.

Acknowledgements This work is supported by the national ANR-JCJC C-MUMS-project (National young investigator project ANR-12-JS03007.01: Control of Multivariable Piezoelectric Microsystems with Minimization of Sensors).

References

1. A. Bergander, W. Driesen, T. Varidel, M. Meizoso, J.M. Breguet, Mobile *cm3*-microrobots with tools for nanoscale imaging and micromanipulation, in *Mechatronics & Robotics* (MechRob 2004), Aachen, Germany, 13–15 Sept 2004, pp. 1041–1047
2. S. Fatikow, T. Wich, H. Hulsen, T. Sievers, M. Jahnisch, Microrobot system for automatic nanohandling inside a scanning electron microscope. *IEEE/ASME Trans. Mechatron.* **12**(3), 244–252 (2007)
3. M. Rakotondrabe, Y. Haddab, P. Lutz, Development, modeling, and control of a micro/nanopositioning 2-DOF stick-slip device. *IEEE/ASME Trans. Mechatron.* **14**(6), 733–745 (2009)
4. Physikinstrumente, Selection guide: linear flexure stages and actuators/nanopositioning systems, http://www.physikinstrumente.com/en/products/nanopositioning/nanopositioning_linear-stage_selection.php (2012)
5. K. Uchino, Piezoelectric ultrasonic motors: overview. *Smart Mater. Struct.* **7**(3), 273–285 (1998)
6. R. Lee, H.L. Li, Development and characterization of a rotary motor driven by anisotropic piezoelectric composite laminate. *Smart Mater. Struct.* **7**(3), 327–336 (1998)
7. S.H. Jun, S.M. Lee, S.H. Lee, H.E. Kim, K.W. Lee, Piezoelectric linear motor with unimorph structure by co-extrusion process. *Sens. Act. A.* **147**(1), 300–303 (2008)
8. G. Binnig, C.F. Quate, Ch. Gerber. Atomic force microscope. *Phys. Rev. Lett.* **56**(9), 930 (1986)
9. R. Perez, J. Agnus, C. Clevy, A. Hubert, N. Chaillet, Modeling, fabrication and validation of a high performance 2-DOF piezoactuator for micromanipulation. *IEEE/ASME Trans. Mechatron.* **10**(2), 161–171 (2005)
10. M. Rakotondrabe, A. Ivan, Development and dynamic modeling of a new hybrid thermo-piezoelectric micro-actuator. *IEEE Trans. Robot.* **26**(6), 1077–1085 (2010)
11. M. Grossard, C. Rotinat-Libersa, N. Chaillet, M. Boukallel, Mechanical and control-oriented design of a monolithic piezoelectric microgripper using a new topological optimization method. *IEEE/ASME Trans. Mechatron.* **1**(14), 32–45 (2009)
12. M. Rakotondrabe, Performances inclusion for stable interval systems, in *ACC (American Control Conference)*, San Francisco CA, USA, June–July 2011, pp. 4367–4372
13. R.E. Moore, *Interval Analysis* (Prentice-Hall, Englewood Cliffs, 1966)
14. L. Jaulin, M. Kieffer, O. Didrit, E. Walter, *Applied Interval Analysis* (Springer, London, 2001)
15. M. Rakotondrabe, *Piezoelectric Cantilevered Structures: Modeling, Control, and Measurement/Estimation Aspects* (Springer, Berlin 2013)
16. R.G. Ballas, *Piezoelectric Multilayer Beam Bending Actuators: Static and Dynamic Behavior and Aspects of Sensor Integration* (Springer, Berlin, 2007)
17. L. Jaulin, E. Walter, Set inversion via interval analysis for nonlinear bounded-error estimation. *Automatica* **29**(4), 1053–1064 (1993)